Part 1: Bypassing the Multi-reference Character of Singlet Molecular Oxygen

Malte F. Jespersen, Solvejg Jørgensen, Matthew S. Johnson, and Kurt V. Mikkelsen*

Department of Chemistry, University of Copenhagen, Universitetsparken 5, DK-2100 Copenhagen, Denmark

E-mail: kmi@chem.ku.dk

Abstract

Ab initio calculations on systems involving singlet molecular oxygen (O_2 ($^1\Delta_g$)) are challenging due to significant multi-reference character arising from the degeneracy of the HOMO and LUMO orbitals in singlet oxygen. Here we investigate the stragegy of bypassing singlet oxygen's multi-reference character by simply adding the experimentally determined singlet/triplet splitting (22.5 kcal/mol) to the triplet ground state of molecular oxygen. This method is tested by calculating rate constants for the reactions of singlet molecular oxygen with furan, 2-methylfuran, 2,5-dimethylfuran, pyrrole, 2-methylpyrrole, 2,5-dimethylpyrrole, and cyclopentadiene. The calculated rate constants are within a factor of 15 compared to experimentally determined rate constants. The results show that energy refinement at the CCSD(T)-F12 level of theory is crucial to achieving accurate results. The reasonable agreement with experimental values validates the bypassing approach which can be used for other systems involving the 1,4-cyclo-addition of singlet oxygen.

Introduction

Molecular oxygen plays an extremely important role in all aspects of aerobic life on earth and its chemistry is closely related to the electronic structure of molecular oxygen.[1,2] Molecular oxygen has three electronic states that, in terms of energy, are located very close to one another. The transitions between the electronic states of molecular oxygen in vacuum are forbidden by the selection rules related to symmetry, spin, orbital angular momentum, and parity.[3] The lowest lying singlet state of molecular oxygen ($^1\Delta_g$) has a life time that is long enough to undergo chemical reactions. The reactivity of singlet oxygen has been used in many applications such as removing pollutants from waste water,[4,5] in photodynamic therapy for treating cancer,[6,7] and as a valuable selective oxidant in organic chemistry.[7,8] Furthermore reaction with singlet oxygen could be an important oxidation path for certain species in the atmosphere and hydrosphere.[9]

Ab initio calculations on systems involving singlet oxygen are challenging due to the inherent multi-reference character, caused by the degeneracy of the HOMO and LUMO orbitals in singlet oxygen and have been the topic of many theoretical studies.[10–14] CASSCF provides a direct way of including the static correlation of the system.[15] CASSCF calculations require selection of an active space which must include the orbitals involved in the reaction, however, selection of the active space is not straightforward. The CASSCF method primarily describes the static correlation of the system. Addition of dynamic corelation to a CASSCF wavefunction is challenging because of the high computational cost and poor scaling with size. Another way of dealing with the multi-reference character of singlet oxygen is the approximate spin projection method where the HOMO and LUMO orbitals are allowed to mix and the electronic energy is corrected on the basis of the spin contmination and the energy of the fist spin contaminat (the triplet state in the case of singlet oxygen). The spin contamination error can be reduced by using the approximate spin projection method[16], however, the results are sensitive to the choice of DFT method.[17–19]

An alternative approach would be to bypass the multi-reference character of singlet oxygen by performing the electronic structure calculation using ground state triplet molecular oxygen, and then adding the experimentally determined energy splitting between the triplet and singlet states of molecular oxygen, as illustrated in Figure 1. For reaction of singlet oxygen with cyclohexadiene[20], this approach has been shown to yield the same qualitative results for B3LYP/6-31G(d) as refining the electronic energy with CASPT2(12e,10o)/6-31G(d). The

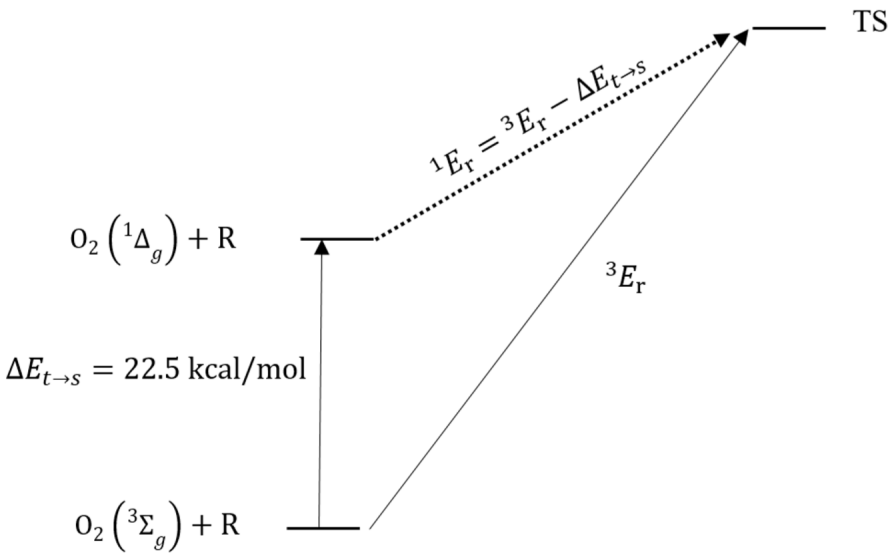

Figure 1: Illustration of the calculations needed to bypass the multi-reference character of singlet oxygen.

accuracy of this approach depends on whether the multi-reference character persists in the TS. While the degeneracy of the HOMO and LUMO orbital in the singlet oxygen moiety is most likely lost in the TS, the transition state might still possess multi-reference character due to close lying molecular orbitals. Bypassing the multi-reference character is by far the most simple and straight forward approach for treating systems containing singlet oxygen.

Discussion of Mechanism

Singlet oxygen is reactive towards many compounds including alkenes and sulfides. If the alkene is a conjugated diene in the cis conformation, singlet oxygen may undergo a 1,4-

cyclo-addition to the alkene via the Diels Alder mechanism to form an endo-peroxide as illustrated in Figure 2. Whether the 1,4-cyclo-addition mechanism of singlet oxygen occurs

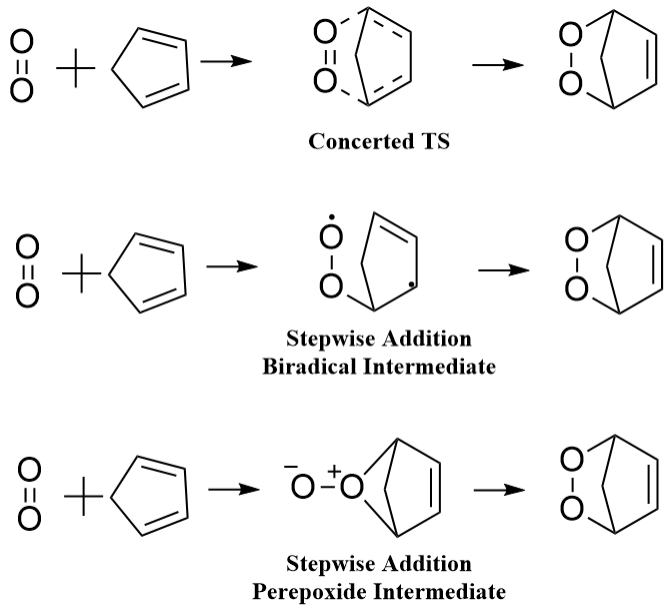

Figure 2: The 1,4-cycloaddition mechanism for the reaction between singlet oxygen and cyclopentadiene.

in a single concerted reaction or as a stepwise addition with a stable intermediate has been debated.[21] Bobrowski et al. examined the 1,4-cycloadition of singlet oxygen to benzene and *cis*-butadiene and found that the benzene reaction proceeds through a concerted mechanism, while the *cis*-butadiene reaction proceeds through a stepwise addition, which also align with earlier MINDO/3 studies.[14] The stepwise mechanism proceded via a biradical intermediate calculated at the level of MCQDPT2/6-31G*//MCSCF/6-31G*. The concerted mechanism was found to have a second order saddle point, 1 kcal/mol higher than the stepwise transition state.[22] However, earlier studies at the MP2/6-31G*//HF/3-21G level of theory found a first order saddle point along the concerted mechanism to be the lowest for the cyclo addition of *cis*-butadiene and singlet oxygen.[23] Sevin et al. studied the cyclo addition of singlet oxygen to 1,3-cyclohexadiene at the CASPT2(12e,10o)/6-31G(d)//B3LYP/6-31G(d) level of theory.[20] In this study the initial energy barrier was found to be 6.5 kcal/mol. They found the reaction to take place via a two-step mechanism at the DFT level, but the energy

barrier of the second transtion state became negative at the CASPT2 level, transforming the mechanism into a concerted but non-synchronous process. Fudickar and Linker found that the reactions of singlet oxygen with anthracenes shift from a step wise mechanism to a concerted one on going from gas phase to acetonitrile solution,[24] indicating the close competition between the two reaction channels. The experimental investigation by Gorman et al. indicates a concerted reaction mechanism for the reaction between singlet oxygen and a range of cyclodienes in toluene.[25]There is experimental evidence that the cyclo-addition in solvent involve a reversibly formed exiplex that might become rate determining at low temperatures.[26]

The goal of this paper is to evaluate different strategies for calculating accurate energy barriers for reactions involving singlet oxygen. Two strategies have been tested. In the first we bypass the multi-reference character of singlet oxygen by performing the energy calculation on the triplet state and then adding the experimentally determined energy difference of 22.5 kcal/mol. The second methodology is based on broken symmetry solution of unrestricted density functional theory calculations (UDFT) where the spin contamination is removed using the approximated spin projected method (AP-UDFT) proposed by Yamaguchi and co-workers.[16] The obtained energy barrriers are used to calculate the rate constants using transition state theory (TST). The rate constant is used to evaluate the energy barriers, by comparing the calculated rate constants with experimentally obtained rate constants. We emphasize that TST is a simple approach, nevertheless it provides valuable insight regarding the reaction kinetics and it is a natural approach yielding results that can be compared with experiment. Arrhenius parameters for the reaction of furan, 2-methylfuran and cyclopentadiene obtained by Ashford and Ogryzlo have similar pre-exponential factors but different activation energies hence the different reactivities of these systems is solely controlled by their activation energies. Based on these findings we argue that TST is a useful approach for testing the performance of different electronic structure theories. The simplicity of the TST model makes the calculation transparent. The calculated rate constants have an expo-

nential dependency on the energy barrier which makes the calculation very sensitive to this parameter. A change of 1 kcal/mol on the energy barrier leads to an approximately 5-fold change in the rate constant, which makes the calculated TST rate constants a useful tool in validating the quality of the energy barriers.

A series of model systems consisting of furan, 2-methylfuran, 2,5-dimethylfuran, pyrrole, 2-methylpyrrole, 2,5-dimethylpyrrole and cyclopentadiene are used to test the method. All the model systems consist of conjugated five membered rings that are able to undergo 1,4-cyclo-addition with singlet oxygen. The gas-phase rate constants for furan, 2-methylfuran, 2,5-dimethylfuran, 2,5-dimethylpyrrole and cyclopentadiene have all been determined experimentally[27,28,29] and serve as validations of the suggested computational strategy.

Computational Method

Gaussian 16[30] is used for all geometry optimizations, employing the aug-cc-pVTZ[31] (AVTZ) basis set and the ωB97XD[32] , B3LYP[33] and M06-2X[34] functionals. The strategy relying on the addition of the experimentally determined singlet/triplet spliting is based on geometry optimizations performed with UDFT and RDFT (RODFT in the case of triplet oxygen), whereas the stragegy based on spin projection is based on geometries optimized with UDFT. Intrinsic reaction coordinate (IRC) calculations are performed to confirm that the TS connects the reactants to the products. Molpro2012[35] is used to perform single point RCCSD(T)-F12a/VDZ-F12[36] energy calculations for obtained geometries. The basis set convergence of the RCCSD(T)-F12a method is tested by comparing the RCCSD(T)-F12a/VDZ-F12 and RCCSD(T)-F12a/VTZ-F12 single point energies performed for the RωB97XD/AVTZ geometries of the furans. If a system possesses significant multi-reference character, RCCSD(T)-F12a calculations might yield unreliable results because of the poor quality of the HF reference wave-function. For example, RCCSD(T)-F12a/VDZ-F12 predicts a singlet/triplet

splitting for molecular oxygen of 28.51 kcal/mol, which is around 6 kcal/mol too high. Two markers are used to judge whether the multi-reference character is still pronounced in the TS, namely the T_1 diagnostics obtained in the RCCSD(T)-F12a calculations, and the spin contamination obtained either from UDFT optimization or from single point UDFT calculations performed at the RDFT optimized geometries. (10e,8o)CASPT2-F12/VTZ-F12 calculations are performed along the reaction coordinate of the furan and singlet molecular oxygen to obtain the energy of the two lowest singlet states and the triplet state. The (10e,8o)CASPT2-F12/VTZ-F12 calculations are performed in Molpro 2012.

The rate constants are calculated using transition state theory:[37]

$$k = L\kappa \frac{k_b T}{h} \frac{Q_{\mathrm{TS}}}{Q_{\mathrm{R}} Q_{^1\mathrm{O}_2}} \mathrm{e}^{-\frac{E_0}{k_B T}}$$

Where k_B, T and h are Boltzmann's constant, the temperature (298 K) and Planck's constant respectively, $\frac{Q_{\mathrm{TS}}}{Q_{\mathrm{R}} Q_{^1\mathrm{O}_2}}$ is the ratio of the partition functions for the TS and the two reactants and E_0 is the electronic energy barrier including zero point vibrational energy (ZPVE). κ is the tunneling correction and is based on the one dimensional Eckart tunneling correction which is calculated from the imaginary frequency of the TS, and the forward and reverse energy barriers.[38] L is the symmetry factor for the reaction and is described in greater detail in the supplementary information (SI).

Result and Discussion

Singlet/triplet splitting in singlet oxygen

It is well known that the singlet/triplet splitting of singlet oxygen is poorly described by a single reference method.[20] This fact is illustrated in Table 1 where RDFT is observed to overestimate the energy spliting by 12.7 kcal/mol whereas UDFT underestimates the energy

splitting by 10.92 kcal/mol. Even the CCSD(T)-F12a/VDZ-F12 method overestimates the energy barrier by around 6 kcal/mol. The UDFT wavefunction can be spin contaminated where higher spin states are mixed in the wavefunction. This is evident from the $\langle S^2 \rangle$ value which is calculated to be around 1 for singlet oxygen, significantly deviating from the expected value of 0 for a pure singlet. Furthermore the lowering of the singlet-triplet splitting from RDFT to UDFT can be attributed to spin contamination of the wavefunction, where the lower lying triplet state is mixed into the UDFT wavefunction. The approximated spin-projection scheme provides a method to remove the contamination coming from the first spin contaminant.[17,16] As seen in Table 1 the approximated spin projected value (AP-UωB97XD/AVTZ) agrees well with the experimentally determined value. The singlet/triplet splittings using AP-UDFT calculated with the functionals B3LYP and M06-2X are shown in Table 1. The difference across all methods is 8.63 kcal/mol; in particular the M06-2X seems to perform poorly. The fact that M06-2X shows the worst performance might be intriguing since this functional has often been chosen for systems involving singlet oxygen using the approximated spin projection method.[18,39]

Table 1: Singlet/triplet splitting calculated using some single reference method

	$\Delta E_{t\to s}$ $\left(\frac{\text{kcal}}{\text{mol}}\right)$
ROωB97XD/AVTZ	35.20
UωB97XD/AVTZ	11.58
AP-UωB97XD/AVTZ	23.16
AP-UB3LYP/AVTZ	20.12
AP-UM06-2X/AVTZ	28.75
UCCSD(T)-F12a/VDZ-F12	28.85
RCCSD(T)-F12a/VDZ-F12	28.51
Exp.	22.5

The large variation among the different DFT functionals indicates that care should be taken when selecting the DFT functional to be used with approximate spin projection methods.

Furan, 2-methylfuran and 2,5-dimethylfuran.

Transition state structures (TS) for the 1,4-cyclo-addition of singlet oxygen to furan, 2-methylfuran and 2,5-dimethylfuran calculated at the ωB97XD/AVTZ level of theory are shown Figure 3. The TS structures are qualitatively the same across the different DFT methods: the TS connects the reactants with the endo-peroxide products in a concerted reaction where both the C-O bonds are formed simultaneously without a stable intermediate between reactants and products. Table 2 shows the energy barriers obtained by performing CCSD(T)-F12a/VDZ-F12 on top of optimized DFT geometries for the reaction of furan, 2-methylfuran and 2,5-dimethylfuran with singlet oxygen. The calculated energy barriers vary within 1.59 kcal/mol across the different DFT methods, showing that similar structures are obtained for the different DFT methods.

Single point CCSD(T)-F12a/VTZ-F12 calculations performed using the ωB97XD/AVTZ geometries are shown in Table 2: these calculations were used to test the effect of expanding the basis set. The energy barriers were seen to decrease by 0.31 kcal/mol or less when increasing the size of the basis set. Some spin contamination was observed for the (U/R)B3LYP/AVTZ and (U/R)M06-2X/AVTZ optimized geometries, but interestingly, no spin contamination was observed in the UωB97XD/AVTZ calculation using the RωB97XD/AVTZ optimized geometry. This might indicate that ωB97XD is more robust in treating the 1,4-cycloaddition reactions. The T_1 diagnostics of the transition states shown in Table 2 are all lower than 0.02 which is often accepted as the upper limit indicating when a single reference method should give reliable results.[40,41] It is accepted that extending the coupled cluster expansion beyond CCSD(T) improves the calculation of multi-reference systems[42] but since both the spin contamination and the T_1 diagnostics were sufficiently low the CCSD(T)-F12a method was deemed to be satisfactory in improving the accuracy of the electronic energies of the DFT optimized transition state structures.

The calculated rates shown in Table 2 are approximately within an order of magnitude compared to the experimentally determined rate constants. Further, the rate constants calculated using CCSD(T)/VTZ-F12 single point energies perform slightly better than the ones calculated using the CCSD(T)/VDZ-F12 energies. It is seen that the calculated rates are generally lower than the experimentally determined rates which is surprising since transition state theory is normally expected to overestimate rate constants where tunneling is not important.[43] This observation might stem from use of the CCSD(T)-F12a/VDZ-F12 method which consistently overestimates the energy in the transition state region, which may indicate that some multi-reference character is still persistent in the TS region. Alternatively, the optimized DFT geometries may not accurately describe the true reaction coordinate, a possibility that is discussed later in this paper

The experimentally determined rate constants are observed to increase in the order $k_{\text{furan}} < k_{\text{2-methylfuran}} < k_{\text{2,5-dimethylfuran}}$, a trend which is clearly captured in the theoretically determined rate constants. Two experimentally determined rate constants were found for 2-methylfuran and they differ by a factor of 4. If the factor of 4 is taken as the general experimental uncertainty for these kinds of systems, the theoretically calculated rates are close to matching the experimental values. It should be mentioned that only standard transition state theory calculations have been performed on the chosen systems, and that more advanced methods would be expected to improve the accuracy of the calculation.

SI Table 2 shows the energy barriers for the furans calculated using the approximate spin projected scheme and the bypassing method (without any CCSD(T)-F12a energy refinement), the energy barries are compared to the CCSD(T)-F12a/VTZ-F12//RωB97XD/AVTZ which was observed to be in good agreement with experiment and hence qualifying it as a benchmark value. The energy barriers are seen to vary within 8.35 kcal/mol and 3.02 kcal/mol across the different functionals using the approximate spin projected and bypassing method respectively. A variation of 8.35 kcal/mol would lead to a change of the TST

rate constant by a factor of 10^6 which is not acceptable. The lower fluctuation observed in the bypassing method indicates that this method is less sensitive to the selection of DFT functional, However, the energy barriers are still 2.07-5.56 kcal/mol higher than the CCSD(T)-F12a/VTZ-F12//RωB97XD/AVTZ value. Hence, the absolute values of the rate constants are expected to be inaccurate but relative values might still be accurate since all the calculated energy barriers are in qualitative agreement with the expected tendency $E_{0,(\text{furan})} > E_{0,(\text{2-methylfuran})} > E_{0,(\text{2,5-dimethylfuran})}$. The energy barriers calculated using AP-UM06-2X are within 1 kcal/mol of the energy barriers obtained at the CCSD(T)-F12a/VTZ-F12//RωB97XD/AVTZ level of theory and the method is observed to be the best performing method for predicting energy barriers for the 1,4-cyclo-addition if energy refinement at the CCSD(T)-F12 level is excluded.

T. Karsili et al. recently studied the 1,4-cycloaddition reaction of singlet molecular oxygen.[44] They performed CASPT2 calculations on approximate reaction surfaces obtained from linear interpolation of internal coordinates. Their calculations suggest that the two degenerate singlet states of molecular oxygen move away from each other in energy as the reaction proceeds towards the transition state, which supports the logic of the bypassing scheme investigated in this study. In their study the triplet and singlet surfaces were found to cross in the region near the transition state. Since the triplet surface is fully repulsive, surface hopping will lead to a quenching of the reaction; the quenching efficiency will be dependent on the spin/orbit coupling. Recent work from the group of Ogilby investigated the quenching mechanism in a solvent where crossing of the singlet and triplet surfaces was a key factor in the quenching mechanism.[45] There are similarities between quenching and chemical reaction and the two processes are in competition with each other. To get a better description of the relevant states along the reaction coordinate we calculated the energy profile of the two lowest singlet states and the triplet state with the CASPT2-F12 method along the reaction coordinate for the reaction between furan and singlet molecular oxygen obtained with the UM06-2X/AVTZ

method. The state averaged (10e,8o)CASSCF reference wavefunction has a bistability point along the reaction coordinate which leads to a discontinuous energy surface, see Supporting Information Figure S2, however the singlet/singlet and singlet/triplet splitting seem not to be affected by this discontinuity (Figure S3). The singlet/triplet splitting calculated at the CASPT2-F12 was utilized as an alternative bypassing scheme where the singlet/triplet splitting was added to the ROCCSD(T)-F12a/VDZ-F12 triplet surface. The ROCCSD(T)-F12a/VDZ-F12 triplet surface should have a well-behaved single reference character, and its multi-reference character is captured using the CASPT2-F12 singlet/triplet splitting. The maximum of this composite reaction surface is slightly shifted towards the reactant region compared to TS on the UM06-2X/AVTZ surface, but the energy difference between the two points is only 0.37 kcal/mol. This indicates that both methods have similar potential energy surfaces i the TS region. The electronic energy barrier is calculated to be 14.79 kcal/mol with the composite method while the UM062X/AVTZ method yields an electronic energy barrier of 17.41 kcal/mol. As shown in table 1 the UM062X/AVTZ method underestimates the energy of the singlet reactants which leads to an overestimation of the electronic energy barrier. The electronic energy barrier calculated with the bypassing scheme in Figure 1 is only 3.43 kcal/mol. Considering the reasonable agreement between experimental data and rate constants calculated in Table 2 it is difficult to believe that the composite method yields an accurate energy barrier for this reaction. Alternatively, the DFT optimized geometries may be a poor description of the true reaction surface. To investigate this possibility CASPT2-F12/VTZ-F12 optimization of the transition state was performed, unfortunately this TS could not be found.

The reasonable performance for the bypassing scheme outlined in Figure 1 with the furan model system encouraged us to look at a range of different systems to test the performance of the method with the strategy that such a test could reveal whether the reasonable agreement with literature was fortuitous or if the method is physically meaningful. Since

the furan results were only marginally affected by the choice of DFT method, and since the ωB97XD/AVTZ calculation did not appear to be affected by spin contamination, the ωB97XD/AVTZ functional was chosen for further optimization, along with M06-2X, since this functional often has been used for similar systems.

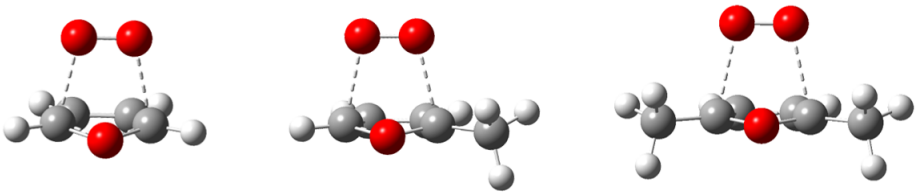

Figure 3: TS structures for the 1,4-cyclo-addition of singlet oxygen on furan (left), 2-methylfuran (middle) and 2,5-dimethylfuran (right), calculated at the RωB97XD/AVTZ level of theory.

Table 2: Spin contaminations, T_1 diagnostic, energy barriers including ZPVE in kcal/mol and rate constants in $\frac{cm^3}{s}$ calculated at CCSD(T)-F12a/VDZ-F12//DFT/AVTZ level of theory using the known singlet/triplet splitting in molecular oxygen.

Furan + $^1O_2$	$\langle S^2 \rangle$	T_1	E_0 $\left(\frac{kcal}{mol}\right)$	k $(\frac{cm^3}{s})$
RM06-2X	0.35	0.016	4.93	3.01×10^{-18}
UM06-2X	0.11	0.017	4.64	6.18×10^{-18}
RB3LYP	0.34	0.017	4.44	8.76×10^{-18}
UB3LYP	0.10	0.018	3.76	3.39×10^{-17}
RωB97XD	0	0.017	4.66	5.49×10^{-18}
RωB97XD[a]	0	0.017	4.35	9.29×10^{-18}
exp.[27]				3.49×10^{-17}
2-Methylfuran + $^1O_2$	$\langle S^2 \rangle$	T_1	E_0 $\left(\frac{kcal}{mol}\right)$	k $(\frac{cm^3}{s})$
RM06-2X	0.48	0.016	2.41	2.15×10^{-16}
UM06-2X	0.13	0.016	1.79	7.51×10^{-16}
RB3LYP	0.45	0.016	1.92	5.93×10^{-16}
UB3LYP	0.11	0.017	0.82	4.09×10^{-15}
RωB97XD	0	0.016	1.99	4.69×10^{-16}
RωB97XD[a]	0	0.016	1.71	7.58×10^{-16}
exp.[27,28]				$(1.66\text{-}5.81)\times10^{-16}$
2,5-Dimethylfuran + $^1O_2$	$\langle S^2 \rangle$	T_1	E_0 $\left(\frac{kcal}{mol}\right)$	k $(\frac{cm^3}{s})$
RM06-2X	0.62	0.015	0.21	9.16×10^{-15}
UM06-2X	0.15	0.016	-0.98	6.22×10^{-14}
B3LYP	-	-	-	
RωB97XD	0	0.015	0.05	1.03×10^{-14}
RωB97XD[a]	0	0.015	-0.12	1.42×10^{-14}
exp.[28]				2.49×10^{-14}

a: Energies obtained from single point CCSD(T)-F12a/VTZ-F12 calculations.

Pyrrole, 2-methylpyrrole and 2,5-dimethylpyrrole.

Transition state structures were found for pyrrole, 2-methylpyrrole and 2,5-dimethylpyrrole (Figure 4). The TS's connect the reactants with the products in a concerted mechanism similar to their furan analogues. As shown in Table 3 the UωB97XD/AVTZ method does not show any spin contamination in the transition state, and the T_1 diagnostics are all lower than 0.02, justifying the use of a single reference method for the transition state. The energy barriers are lowered when a hydrogen is exchanged with a methyl-group in the pyrrol moiety,

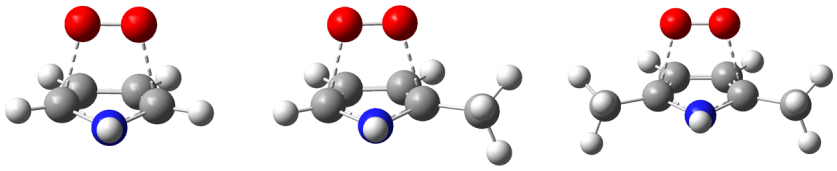

Figure 4: TS structure of pyrrol (left), 2-methylpyrrol (middle) and 2,5-dimethylpyrrol (right), calculated at RωB97XD/AVTZ level of theory.

in qualitative agreement with the furan system. The energy barrier is observed to become negative for the 2-methylpyrrol and 2,5-dimethylpyrrol. Transition state theory breaks down when the energy barrier becomes negative, and ideally other methods should be applied when calculating such rate constants, however, for the sake of comparison the rate constants are calculated using traditional transition state theory (without tunneling correction) for systems with negative barriers. Experimentally determined rate constants have to our knowledge only been determined for the 2,5-dimethylpyrrole reaction 1.66×10^{-13} $\frac{\mathrm{cm}^3}{\mathrm{s}}$. The calculated rate constants are 20-60 times higher than the experimentally determined ones. The fact that the calculated rates are faster than experiment, can be attributed to the negative energy barriers which leads to a non-physical enhancement of the rate constant.

The negative energy barrier could be explained by the existence of a pre-reactive exiplex, with a lower energy than the transition state. An exiplex was found in the Uω97XD/AVTZ optimization, however the Uω97XD/AVTZ wave function was found to be heavily spin contaminated with $\langle S^2 \rangle \approx 1$. The heavy spin contamination in this range of the reaction surface prohibits us utilizing the bypassing scheme outlined in Figure 1. We conclude that a full multi-reference treatment is necessary for including the exiplex in the kinetic model. Reaction enthalpies close to zero are often found for reactions of singlet oxygen in solution, in this case it is found that it is the entropy rather than the enthalpy which controls the reactivity of singlet oxygen.[25]

Table 3: Spin contaminations, T_1 diagnostic, energy barriers including ZPVE in kcal/mol and rate constants in $\frac{cm^3}{s}$ calculated at CCSD(T)-F12a/VDZ-F12//DFT/AVTZ level of theory using the known singlet/triplet splitting in molecular oxygen.

pyrrole + $^1O_2$	$\langle S^2 \rangle$	T_1	E_0 $\left(\frac{kcal}{mol}\right)$	k $(\frac{cm^3}{s})$	exp.
RωB97XD	0	0.017	2.57	1.47×10^{-16}	
RM06-2X	0	0.016	2.88	8.81×10^{-17}	
2-Methylpyrrole + $^1O_2$	$\langle S^2 \rangle$	T_1	E_0 $\left(\frac{kcal}{mol}\right)$	k $(\frac{cm^3}{s})$	exp.
RωB97XD	0	0.016	-0.70	2.95×10^{-14}	
RM06-2X	0.11	0.015	-0.37	1.79×10^{-14}	
UM06-2X	0.02	0.015	-0.44	1.92×10^{-14}	
2,5-Dimethylpyrrole + $^1O_2$	$\langle S^2 \rangle$	T_1	E_0 $\left(\frac{kcal}{mol}\right)$	k $(\frac{cm^3}{s})$	exp.[29]
RωB97XD	0	0.015	-3.58	3.55×10^{-12}	1.66×10^{-13}
RM06-2X	0.44	0.014	-3.70	5.58×10^{-12}	
UM06-2X	0.07	0.015	-3.43	3.19×10^{-12}	

Cyclopentadiene

Cyclopentadiene is chosen because experimental data is available for this system and it is expected to follow a 1,4-cycloaddition mechanism as for the furan and pyrrole derivates. The optimized transition state obtained at the RωB97XD/AVTZ level of theory is shown

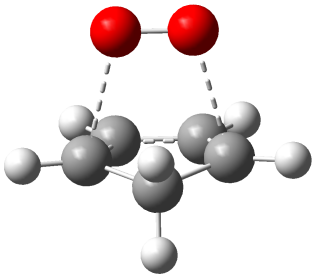

Figure 5: TS structure of cyclopentadiene calculated at RωB97XD/AVTZ level of theory.

in Figure 5. The obtained transition states connect the reactants directly to the product in a concerted reaction. Table 4 shows that no spin contamination is observed for the RωB97XD/AVTZ optimized TS and the T_1 diagnostics are lower than 0.02. Again, the multi-reference character is lost in the transition state when optimizing using the RωB97XD/AVTZ

method. Two different TS's were optimized using the UωB97XD/AVTZ method. One of them is identical to the TS obtained with RωB97XD/AVTZS, and the other is more product like, with shorter C-O bonds. The second transition state possess some spin contamination with a $\langle S^2 \rangle$ value of 0.27. It was not possible to find a second TS at the RωB97XD/AVTZ level of theory, so we conclude that the second TS is an artefact arising from spin contamination of the wavefunction, which leads to an artificial lowering of the energy over some part of the potential energy surface. The TS found at the RM06-2X/AVTZ level of theory is more reactant-like compared to the one optimized with the UM06-2X/AVTZ method. Here we again observe the trend seen in ωB97XD/AVTZ where the RDFT finds an earlier transition state compared to UDFT. This general trend is also observed for the furan and pyrrole derivatives. The excellent agreement with experimental rates observed for the UωB97XD/AVTZ calculated rates may simply be due to cancellation of errors. The RωB97XD/AVTZ calculated rate constant is 15 times slower than the experimentally determined one. The RωB97XD/AVTZ calculated rate constant shows the worst agreement with experiment, however from a computational point of view, it seems to be the most reliable result since no spin-contamination is observed for the TS and the T_1 diagnostic is reasonably low.

Table 4: Spin contaminations, T_1 diagnostic, energy barriers including ZPVE in kcal/mol and rate constants in $\frac{\text{cm}^3}{\text{s}}$ calculated at CCSD(T)-F12a/VDZ-F12//DFT level of theory using the known singlet/triplet splitting in molecular oxygen.

Cyclopentadiene + $^1O_2$	$\langle S^2 \rangle$	T_1	E_0 $\left(\frac{\text{kcal}}{\text{mol}}\right)$	k $\left(\frac{\text{cm}^3}{\text{s}}\right)$
RωB97XD	0	0.015	3.87	3.90×10^{-17}
RM06-2X	0.61	0.015	2.96	1.14×10^{-16}
UωB97XD	0.26	0.016	2.06	5.33×10^{-16}
UM06-2X	0.25	0.016	3.11	1.87×10^{-16}
exp.[27]				5.81×10^{-16}

Temperature Dependency

The temperature dependency of the calculated k_{TST} were obtained and compared to those obtained by Ashford and Ogryzlo to validate the quality of the calculated rate constants. As shown in SI Figure 5 the calculated rates seem to predict the temperature dependencies resonably well in the interval (298 K - 500 K). In SI Figure 6 the energy barriers are manually changed by less than 1.5 kcal/mol so the calculated rate constants match the experimental ones at 298 K. When the temperature is increased to 500 K the experimentally determined rate constant increases to approximately twice the calculated one. This result shows that TST performs reasonably well in predicting the temperature dependency, but tends to underestimate it. It also shows that the activation barrier for these systems is the most important parameter to be determined in order to obtain accurate rate constants.

Conclusion

The rate constants for the reactions between singlet oxygen and 7 different reactants are calculated by bypassing the multi-reference character of singlet oxygen by performing the electronic structure calculations on the triplet state of molecular oxygen and then adding the experimentally determined energy difference between the two states to obtain the effective energy of the singlet state. All the optimized transition states have low T_1 diagnostics indicating that the inherent multi-reference character of singlet oxygen is lost in the transition state, since the degeneracies of the molecular orbitals are lost when the transition states are reached. The calculated rates are all within a factor of 15 of the experimentally determined rate constants (excluding the non-physical results obtained from 2,5-dimethylpyrrole). We believe that the accuracy could be further improved by going beyond the transition state approximation.

We have tried to perform variational transition state theory calculations on the system to go beyond TST, however, the poor description of singlet oxygen by (R/U)DFT becomes

more pronounced when going from the transition state towards reactants. This fact has prevented us from obtaining converged reaction paths at the VTST level of theory, and we are working to resolve this issue.

Most of the calculated rate constants were lower than the experimentally determined rate constants which could indicate that there is a systematic error in either the calculation or the experiments. Care should be taken when selecting the DFT method for optimizations. UDFT seems to be influenced by spin contamination and artificial TS's can arise as a result of the spin contamination. The agreement with experimentally determined rates is reasonable for both RDFT and UDFT and we recommend using the RωB97XD functional to optimize transition states for 1,4-cycloaddition reactions involving singlet oxygen, since this functional seems to be the least spin contaminated. We also recommend refining the energy with a single point CCSD(T)-F12a/VDZ-F12 calculation since the pure DFT energies show huge variations across different functionals. We do not recommend using the approximate spin projection method in connection with DFT energies for calculating rate constants for systems involving singlet molecular oxygen, since the energy variation is up to 8.16 kcal/mol across different DFT functionals, compared to 2 kcal/mol when the energy is refined with CCSD(T)-F12a/VDZ-F12 single point calculations. The approximate spin projected energy barriers at M06-2X/AVTZ level of theory were in best agreement with the CCSD(T)-F12a/VDZ-F12 barrier, so we recommend this functional when an approximate spin projected method is needed for systems involving singlet molecular oxygen.

The proposed bypassing of the multi reference character of singlet oxygen yields a straightforward methodology for calculating rate constants without the complication of multi-reference calculations. The reasonable performance for calculating rate constants for the various methods and with different chemical systems show that the multi-reference character in singlet oxygen can be effectively bypassed by performing the calculations with the triplet state of

molecular oxygen and adding the experimentally determined singlet/triplet energy splitting to obtain the energy of singlet oxygen.

Supporting Info

Symmetry numbers. Approximate spin projection method. IRC calculations. Temperature dependency of selected rate constant. Geometries of all stationary points calculated with ωB97XD/AVTZ.

Acknowlegdements

This work was supported by the Center for Exploitation of Solar Energy, Department of Chemistry, University of Copenhagen, Denmark.

References

(1) Lane, N. *Oxygen: The Molecule that Made the World*, 1st ed.; Oxford University Press: Oxford, 2002.

(2) Bregnhøj, M.; Westberg, M.; Minaev, B. F.; Ogilby, P. R. Singlet oxygen photophysics in liquid solvents: converging on a unified picture. *Acc. Chem. Res.* **2017**, *50*, 1920–1927.

(3) Herzberg, G. *Molecular Spectra and Molecular Structure. I Spectra of Diatomic Molecules*, 2nd ed.; Van Nostrand Reinhold: New York, 1950.

(4) Gerdes, R.; Wöhrle, D.; Spiller, W.; Schneider, G.; Schnurpfeil, G.; Schulz-Ekloff, G. Photo-oxidation of phenol and monochlorophenols in oxygen-saturated aqueous solutions by different photosensitizers. *Journal of Photochemistry and Photobiology A: Chemistry* **1997**, *111*, 65–74.

(5) Iliev, V.; Prahov, L.; Bilyarska, L.; Fischer, H.; Schulz-Ekloff, G.; Whrle, D.; Petrov, L. Oxidation and photooxidation of sulfide and thiosulfate ions catalyzed by transition metal chalcogenides and phthalocyanine complexes. *J. Mol. Catal. A: Chem.* **2000**, *151*, 161 – 169.

(6) Bonnett, R. Photosensitizers of the porphyrin and phthalocyanine series for photodynamic therapy. *Chem. Soc. Rev.* **1995**, *24*, 19–33.

(7) DeRosa, M. C.; Crutchley, R. J. Photosensitized singlet oxygen and its applications. *Coord. Chem. Rev.* **2002**, *233*, 351–371.

(8) Wasserman, H. H.; Ives, J. L. Singlet oxygen in organic synthesis. *Tetrahedron* **1981**, *37*, 1825–1852.

(9) Faust, B. C.; Allen, J. M. Aqueous-phase photochemical sources of peroxyl radicals and singlet molecular oxygen in clouds and fog. *J. Geophys. Res.: Atmos* **1992**, *97*, 12913–12926.

(10) Yamaguchi, K.; Yamanaka, S.; Shimada, J.; Isobe, H.; Saito, T.; Shoji, M.; Kitagawa, Y.; Okumura, M. Extended HartreeFock theory of chemical reactions. IX. Diradical and perepoxide mechanisms for oxygenations of ethylene with molecular oxygen and iron-oxo species are revisited. *Int. J. Quantum Chem.* **2009**, *109*, 3745–3766.

(11) Harding, L. B.; Goddard III, W. A. The mechanism of the ene reaction of singlet oxygen with olefins. *J. Am. Chem. Soc* **1980**, *102*, 439–449.

(12) Alberti, M. N.; Orfanopoulos, M. Unraveling the mechanism of the singlet oxygen ene reaction: recent computational and experimental approaches. *Chem. Eur* **2010**, *16*, 9414–9421.

(13) Singleton, D. A.; Hang, C.; Szymanski, M. J.; Meyer, M. P.; Leach, A. G.; Kuwata, K. T.; Chen, J. S.; Greer, A.; Foote, C. S.; Houk, K. Mechanism of ene

reactions of singlet oxygen. A two-step no-intermediate mechanism. *J. Am. Chem. Soc* **2003**, *125*, 1319–1328.

(14) Dewar, M. J.; Thiel, W. MINDO/3 study of the addition of singlet oxygen (1. DELTA. gO2) to 1, 3-butadiene. *J. Am. Chem. Soc* **1977**, *99*, 2338–2339.

(15) Schmidt, M. W.; Gordon, M. S. The construction and interpretation of MCSCF wavefunctions. *Annu. Rev. Phys. Chem.* **1998**, *49*, 233–266.

(16) Yamanaka, S.; Kawakami, T.; Nagao, H.; Yamaguchi, K. Effective exchange integrals for open-shell species by density functional methods. *Chem. Phys. Lett.* **1994**, *231*, 25–33.

(17) Saito, T.; Nishihara, S.; Kataoka, Y.; Nakanishi, Y.; Kitagawa, Y.; Kawakami, T.; Yamanaka, S.; Okumura, M.; Yamaguchi, K. Reinvestigation of the reaction of ethylene and singlet oxygen by the approximate spin projection method. Comparison with multireference coupled-cluster calculations. *J. Phys. Chem. A* **2010**, *114*, 7967–7974.

(18) Al-Nuairat, J.; Altarawneh, M.; Gao, X.; Westmoreland, P. R.; Dlugogorski, B. Z. Reaction of aniline with singlet oxygen (O2 1Δg). *J. Phys. Chem. A* **2017**, *121*, 3199–3206.

(19) Saito, T.; Nishihara, S.; Kataoka, Y.; Nakanishi, Y.; Matsui, T.; Kitagawa, Y.; Kawakami, T.; Okumura, M.; Yamaguchi, K. Transition state optimization based on approximate spin-projection (AP) method. *Chem. Phys. Lett.* **2009**, *483*, 168–171.

(20) Sevin, F.; McKee, M. L. Reactions of 1, 3-cyclohexadiene with singlet oxygen. A theoretical study. *J. Am. Chem. Soc.* **2001**, *123*, 4591–4600.

(21) Leach, A. G.; Houk, K. Diels–Alder and ene reactions of singlet oxygen, nitroso compounds and triazolinediones: transition states and mechanisms from contemporary theory. *Chem. Commun.* **2002**, 1243–1255.

(22) Bobrowski, M.; Liwo, A.; Odziej, S.; Jeziorek, D.; Ossowski, T. CAS MCSCF/CAS MCQDPT2 study of the mechanism of singlet oxygen addition to 1,3-butadiene and benzene. *J. Am. Chem. Soc.* **2000**, *122*, 8112–8119.

(23) McCarrick, M. A.; Wu, Y. D.; Houk, K. Hetero-Diels-Alder reaction transition structures: reactivity, stereoselectivity, catalysis, solvent effects, and the exo-lone-pair effect. *J. Org. Chem.* **1993**, *58*, 3330–3343.

(24) Fudickar, W.; Linker, T. Theoretical insights into the effect of solvents on the [4+ 2] cycloaddition of singlet oxygen to substituted anthracenes: A change from a stepwise process to a concerted process. *J. Phys. Org. Chem.* **2019**, *32*, e3951.

(25) Gorman, A.; Lovering, G.; Rodgers, M. The entropy-controlled reactivity of singlet oxygen (1. DELTA. g) toward furans and indoles in toluene. A variable-temperature study by pulse radiolysis. *J. Am. Chem. Soc* **1979**, *101*, 3050–3055.

(26) Gorman, A.; Hamblett, I.; Lambert, C.; Spencer, B.; Standen, M. Identification of both preequilibrium and diffusion limits for reaction of singlet oxygen, O2 (1. DELTA. g), with both physical and chemical quenchers: variable-temperature, time-resolved infrared luminescence studies. *J. Am. Chem. Soc* **1988**, *110*, 8053–8059.

(27) Ashford, R.; Ogryzlo, E. Arrhenius parameter for some gas-phase cycloaddition reactions of singlet molecular oxygen. *Can. J. Chem.* **1974**, *52*, 3544–3548.

(28) Huie, R. E.; Herron, J. T. Kinetics of the reactions of singlet molecular oxygen (O21Δg) with organic compounds in the gas phase. *Int. J. Chem. Kinet.* **1973**, *5*, 197–211.

(29) Fiedler, E.; Hack, W. The reaction of 2, 5-dimethylpyrrole with O2 (a1Δg) in the gas phase. *Int. J. Chem. Kinet.* **1991**, *23*, 925–939.

(30) Frisch, M. J.; Trucks, G. W.; Schlegel, H. B.; Scuseria, G. E.; Robb, M. A.; Cheese-

man, J. R.; Scalmani, G.; Barone, V.; Petersson, G. A.; Nakatsuji, H.; Li, X.; et al., Gaussian 16, Revision A.03. 2016; Gaussian Inc. Wallingford CT.

(31) Kendall, R. A.; Dunning Jr, T. H.; Harrison, R. J. Electron affinities of the first-row atoms revisited. Systematic basis sets and wave functions. *J. Chem. Phys* **1992**, *96*, 6796–6806.

(32) Chai, J. D.; H. Gordon, M. Long-range corrected hybrid density functionals with damped atom-atom dispersion corrections. *Phys. Chem. Chem. Phys.* **2008**, *10*, 6615–6620.

(33) Becke, A. D. Density-functional thermochemistry. III. The role of exact exchange. *J. Chem. Phys.* **1993**, *98*, 5648–5652.

(34) Zhao, Y.; Truhlar, D. G. The M06 suite of density functionals for main group thermochemistry, thermochemical kinetics, noncovalent interactions, excited states, and transition elements: two new functionals and systematic testing of four M06-class functionals and 12 other functionals. *Theory. Chem. Acc.* **2008**, *120*, 215–241.

(35) Werner, H.-J.; Knowles, P. J.; Knizia, G.; Manby, F. R.; Schütz, M.; Celani, P.; Györffy, W.; Kats, D.; Korona, T.; Lindh, R.; et al., MOLPRO, version 2012.1, a package of ab initio programs. 2012; Cardiff, UK.

(36) Knizia, G.; Adler, T. B.; Werner, H.-J. Simplified CCSD (T)-F12 methods: Theory and benchmarks. *J. Chem. Phys* **2009**, *130*, 054104.

(37) Eyring, H. The activated complex in chemical reactions. *J. Chem. Phys* **1935**, *3*, 107–115.

(38) Eckart, C. The penetration of a potential barrier by electrons. *Phys. Rev.* **1930**, *35*, 1303.

(39) Al-Nuairat, J.; Dlugogorski, B. Z.; Gao, X.; Zeinali, N.; Skut, J.; Westmoreland, P. R.; Oluwoye, I.; Altarawneh, M. Reaction of phenol with singlet oxygen. *Phys. Chem. Chem. Phys.* **2019**, *21*, 171–183.

(40) Lee, T. J.; Taylor, P. R. A diagnostic for determining the quality of single-reference electron correlation methods. *Int. J. Quantum Chem.* **1989**, *36*, 199–207.

(41) Goldsmith, C. F.; Klippenstein, S. J.; Green, W. H. Theoretical rate coefficients for allyl+ HO 2 and allyloxy decomposition. *Proc. Combust. Inst.* **2011**, *33*, 273–282.

(42) Chan, B.; Radom, L. W3X: A cost-effective post-CCSD (T) composite procedure. *J. Chem. Theory Comput.* **2013**, *9*, 4769–4778.

(43) Truhlar, D. G.; Garrett, B. C. Variational transition-state theory. *Acc. Chem. Res.* **1980**, *13*, 440–448.

(44) Karsili, T. N.; Marchetti, B. Oxidative addition of singlet oxygen to model building-blocks of the aerucyclamide a peptide: a first principles approach. *J. Chem. Phys A* **2019**,

(45) Thorning, F.; Jensen, F.; Ogilby, P. R. Modeling the effect of solvents on nonradiative singlet oxygen deactivation: going beyond weak coupling in intermolecular electronic-to-vibrational energy transfer. *J. Phys. Chem. B* **2020**, *124*, 2245–2254.